Journal of Chromatography B, 902 (2012) 78–83

Contents lists available at SciVerse ScienceDirect

Journal of Chromatography B

journal homepage: www.elsevier.com/locate/chromb

Diffusion Split-Flow Thin Cell (SPLITT) system for protein separations

Srinivas Merugu[a,1], Himanshu J. Sant[b,1], Bruce K. Gale[c,*]

[a] State of Utah Center of Excellence for Biomedical Microfluidics, Department of Electrical Engineering, University of Utah, 50 S. Central Campus Drive, Rm. 2110, Salt Lake City, UT 84112, United States
[b] State of Utah Center of Excellence for Biomedical Microfluidics, Department of Bioengineering, University of Utah, 50 S. Central Campus Drive, Rm. 2110, Salt Lake City, UT 84112, United States
[c] State of Utah Center of Excellence for Biomedical Microfluidics, Department of Mechanical Engineering, University of Utah, 50 S. Central Campus Drive, Rm. 2110, Salt Lake City, UT 84112, United States

ARTICLE INFO

Article history:
Received 26 October 2011
Accepted 24 June 2012
Available online 1 July 2012

Keywords:
Field flow fractionation
Microfluidics
Split-Flow Thin Cell
Dialysis
Continuous separation

ABSTRACT

A diffusion Split-Flow Thin Cell (SPLITT) system was used to partially remove small peptides such as β2 microglobulin (β2M) and parathyroid hormone (PTH) in a continuous manner from an input flow stream while preserving most (over 97%) of the larger protein in the sample, such as albumin. To help determine the operating conditions for this work, a two-dimensional numerical model based on the Navier–Stokes equation and convection–diffusion equations was developed for diffusional SPLITT using COMSOL multiphysics software (COMSOL Inc., MA). These simulations were used to obtain the relationship between important operational parameters and the purification efficiency for proteins of interest. The diffusion-based SPLITT system was fabricated using xurography and was used to demonstrate protein purification based on the differences in size or diffusion coefficient of the sample. The results obtained from the experiments are compared with the mathematical model and show good agreement, while the variations between these results are discussed. The results show that significant portions of small peptides (>25%) can be removed while preserving larger proteins (up to 95%) in the carrier stream. A potential application of this technique is to be used as an additional step in kidney dialysis to remove toxins that are not effectively removed by current dialysis protocols.

1. Introduction

Split-Flow Lateral-Transport Thin Cell (SPLITT) is a separation method related to the Field-Flow Fractionation (FFF) family of techniques [1,2]. SPLITT separates particles continuously and can achieve high throughput particle separations [3,4]. SPLITT channels consist of a thin ribbon like fluid channel with two inlets and two outlets with thin splitter separating both of the inlets and outlets as shown in Fig. 1. The splitter is provided to prevent undesirable mixing at the two inlets and outlets and to allow a smooth transition of both sample and carrier across these ports. In normal SPLITT operation, a field is applied across the thin dimension of the channel to force particles to migrate across the channel. A number of subtypes of SPLITT that are differentiated by the type of the field have been reported. Fields such as gravitational [5], centrifugal [6,7], electric [8,9] and magnetic [10,11] have been used to separate particles based on different physiochemical properties like molecular weight, size, electrophoretic mobility, magnetic permittivity, and density. The flow arrangement depicted in Fig. 1 generates the *transport mode* of separation. In this figure, the inlet splitting plane (ISP) is an imaginary plane isolating the sample entering from *inlet a′* and the carrier from *inlet b′*. Similarly, the outlet splitting plane (OSP) divides the solutions eluting from the outlets. Changing the inlet and outlet flow rates can control the distance between the ISP and OSP, known as the transport region. Samples that cross the transport region under the influence of the field will elute from *outlet b* whereas other particles would elute from *outlet a*. The relative flow rates and the field strength determine the resolution of particle separations in SPLITT for given samples.

Of the different SPLITT subtypes, diffusional SPLITT is the simplest to use, as no applied field is required. Diffusional SPLITT is very effective at dividing samples with significant differences in diffusivity or molecular weights. For diffusional SPLITT operation, parameters such as *diffusion distance* and the *time* spent by the sample in the channel govern the separation of the samples with different diffusion coefficients. For example, if we consider a mixture of two different particle types (such that particle A has a smaller diffusion coefficient than particle B) that are passed through *inlet a′* (as shown in Fig. 1) with flow rates maintained

* Corresponding author. Tel.: +1 801 585 5944; fax: +1 801 585 9826.
E-mail addresses: merugu_s@yahoo.com (S. Merugu), himanshu.sant@utah.edu (H.J. Sant), gale@eng.utah.edu (B.K. Gale).
URL: http://www.mems.utah.edu (B.K. Gale).
[1] Tel.: +1 801 585 3176; fax: +1 801 585 9826.

1570-0232/$ – see front matter © 2012 Elsevier B.V. All rights reserved.
http://dx.doi.org/10.1016/j.jchromb.2012.06.029

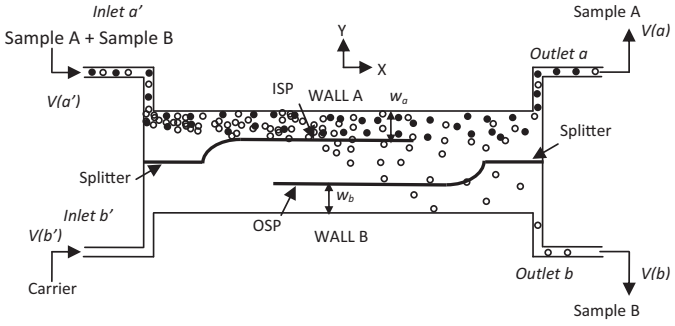

Fig. 1. A schematic showing the principle of SPLITT for the transport mode of operation. ISP and OSP stand for imaginary planes called the inlet splitting plane and outlet splitting plane respectively.

such that only some of particle B has enough time to diffuse across the transport region and elute from *outlet b*. Under such conditions, only a very small amount of the particles with lower diffusion coefficients will elute from *outlet b*, whereas a significant amount of particle B elutes from *outlet b*. Thus, particle A has been purified substantially by removal of only particle B.

Diffusional SPLITT can be efficiently used to remove or purify proteins with a substantial difference in molecular weights very quickly even without the use of any external field. An external field added to the diffusion process may allow for additional specificity and speed. In any case strong fields such as large electric fields, high temperature gradients and high ionic strength buffers can cause problems in macromolecule processing as they may result in irreversible structural damage to delicate samples. These risks are especially important in an application such as blood purification, which is of special interest in this work.

Typically, hemodialysis is used to aid patients with kidney failure that need to remove salt, excess water and a host of other small and middle-sized molecules. A number of reports have suggested that hemodialysis does not completely remove certain toxins, such as β2 microglobulin (β2M) and parathyroid hormone (PTH), from uremic blood. Requirements for smaller pore sizes than typical of current dialysis membranes and/or affinity for these toxins for other biological materials are reasons these molecules are not removed. If the pore size of the dialysis membrane is increased, it may result in loss of important proteins, such as albumin, to the dialysate. β2M and PTH fall in this class of moderately sized peptides with molecular weights of 11.6 kDa [12] and 9.42 kDa [13] respectively. The gradual accumulation of β2M, a serum protein in osteoarticular tissue, causes a disease known as β-2-Microglobulin-Amyloidosis. There are many reports confirming that long term dialysis patients are affected by amylodosis [14] and it can be fatal. The incidence of amylodiosis is estimated to be greater than 95% in patients on dialysis for more than 15 years [15]. European studies suggest 20% of patients undergoing hemodialysis for 2–4 years have been diagnosed for amylodiosis. These numbers rise to 100% for people undergoing hemodialysis for 13 years [16]. PTH accumulation in dialysis patients has been related to carpal tunnel syndrome [17], high blood pressure [18] and secondary hyperparathyroidism [19].

SPLITT-based techniques have the potential to increase the removal of these important toxins that cannot be removed using normal-hemodialysis protocols. The characterization of diffusional SPLITT reported here is a possible first step towards the development of a high-speed toxin removal system.

Diffusional SPLITT can also be used for measuring the diffusivity of particles if a robust mathematical model is developed for it. A good mathematical model can also be used for finding experimental parameters for which good purification can be obtained without running extensive experiments. As this is a new topic for research, there is no adequate 2-dimensional mathematical model for diffusional SPLITT. In this paper, a new two dimensional model for diffusional SPLITT is developed using commercially available software called COMSOL. COMSOL was chosen as it is a multiphysics software package that can solve both fluid dynamics and convection–diffusion problems simultaneously.

2. Theory

The theory behind diffusion SPLITT is developed by Giddings et al. [20] and here only a few details are provided to refresh the knowledge of the reader. The operation of diffusion SPLITT is pictorially shown in Fig. 1, where flow through inlet a′ ($v(a')$) results in stream lamina w_a, which contains the sample or input material. $v(a')$ is usually kept smaller than the carrier flow from inlet b′ ($v(b')$) to obtain a higher resolution. The theory behind SPLITT was simplified by Giddings by conceptualizing two imaginary planes separating the inlet flows and outlet flows. The plane which separates inlet flows is called the inlet splitting plane (ISP) and the plane which separates the outlet flows is called the outlet splitting plane (OSP). The region separating the ISP and the OSP is called the transport region and the particles that move across this region will elute from outlet *b* whereas particles which do not cross this region elute from *outlet a*.

The relation between volumetric flow rates and w_a is given by

$$\frac{V(a')}{V} = 3\left(\frac{w_a}{w}\right)^2 - 2\left(\frac{w_a}{w}\right)^2, \tag{1}$$

where V is the total flow rate, which is equal to the sum of the inlet flow rates or the sum of the outlet flow rates and w is the width of the channel.

Eq. (1) can be solved to give

$$\left(\frac{w_a}{w}\right) = \frac{1}{2} + \sin\left(\frac{\theta}{3}\right), \tag{2}$$

where

$$\sin\theta = 2\left(\frac{V(a')}{V}\right) - 1. \tag{3}$$

Eq. (2) gives the position of the ISP based on volumetric flowrates at the inlet. Similarly, one can also calculate the position of OSP from outlet flowrates. Giddings et al. [20] used the simplified convection–diffusion equation to solve for the particle concentration inside the channel. The standard convection–diffusion equation is given by

$$\frac{\partial C}{\partial t} + \nabla\cdot(-D\nabla C + cu) = 0, \tag{4}$$

where c is the concentration of the analyte, D is the diffusion coefficient of the analyte and u is the velocity vector. This equation forms the basis of the COMSOL modeling effort.

3. Methods

3.1. Modeling

The Navier–Stokes and convection–diffusion equations were solved using COMSOL multiphysics software to simulate both the fluid flow and the sample transport in the channel geometry shown in Fig. 2. Transport in the breadth direction of the SPLITT channel (denoted as the z-direction in Fig. 2) is constant along the length of the channel and hence, a 2-dimensional model is sufficient. Fig. 2 shows the transport processes occurring in the SPLITT channel and boundary and subdomain conditions used for the simulations. A finer mesh is used in the middle of the SPLITT channel where the later diffusion processes occur after the sample passes

Table 1
Values for the parameters used in the numerical simulations.

Parameter	Range	Units
Diffusion coefficient	0.61×10^{-10}, 1.40×10^{-10}, 1.53×10^{-10}	m^2/s
Inlet flow rate a'	5.51–99.14	mm/s
Inlet flow rate b'	11.02–99.14	mm/s
Outlet flow rate a	11.02–99.14	mm/s
Outlet flow rate b	11.02–99.14	mm/s

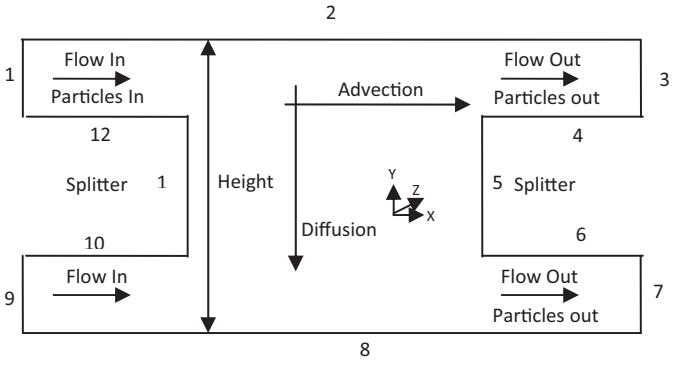

Fig. 2. An overview of the various transport phenomena occurring in the diffusional SPLITT system: the primary contributors are advection due to fluid flow in the channel and diffusion, which occurs in all directions, but because of the small channel dimension in the *y*-direction, has the most impact in that direction.

the splitter location; otherwise a coarse mesh is used in the channel ends for efficient computation. The sample concentration was assumed to be 3 mg/ml in the inlet sample stream (note that this concentration is sufficient for detection of the proteins and that the concentration has minimal effect on the overall results). The species used in the simulations and their diffusion coefficients (D) were: HSA (0.61×10^{-10} m^2/s) [21], β2M (1.53×10^{-10} m^2/s) [22] and PTH (1.40×10^{-10} m^2/s) [23].

The flow velocities, computed by solving the Navier–Stokes equations, were stored and used to solve the convection–diffusion equation and to map the sample transport and dispersion due to the fluid flow for a given channel geometry. Table 1 shows the values of various parameters used in simulations.

The boundary conditions for the channel geometry are shown in Fig. 2 and Navier–Stokes and convection–diffusion equations are listed in Table 2.

3.2. Fabrication

The SPLITT system has been fabricated similar to the diffusion SPLITT described by Giddings et al. [20] with a few modifications to improve the flow distribution and reliability of the channel. Glass plates of 6.4 mm thickness were used as the walls of the channel. Inlet and outlet ports, 34 cm apart were created in the glass with a silicon carbide drill bit of 1.5875 mm diameter. The SPLITT channel

Table 2
Boundary conditions used in numerical modeling.

Boundaries as shown in Fig. 2	Navier–Stokes boundary condition	Convection–diffusion boundary condition
2, 4, 5, 6, 8, 10, 11, 12	No slip	Insulation: $n \cdot (-D\nabla c + cu) = 0$
1	Inlet (constant velocity)	Concentration = C_0 (0.0455 mol/m^3)
9	Inlet (constant velocity)	Concentration = 0
3	Outlet (constant velocity)	Convective flux: $n \cdot (-D\nabla c) = 0$
7	Outlet with pressure = 0	Convective flux: $n \cdot (-D\nabla c) = 0$

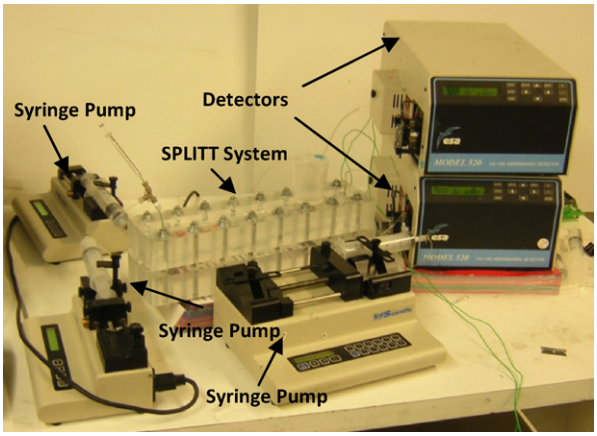

Fig. 3. Picture of the experimental setup.

consists of two flow channels that are separated by a rectangular splitter to avoid mixing and recirculation at the channel ends.

A Mylar sheet of 0.1 mm thickness and a polyethylene sheet of 0.25 mm thickness were patterned using a knife plotter (Graphtec America, FC 5100-75) (xurography) to obtain channels and the splitter respectively. The overall length of the splitting region is 20 cm. The channels were attached to either sides of the splitter using 25 μm thick tapes with adhesive on both sides (9019, 3M) to facilitate proper alignment of the laminates. The total thickness of the SPLITT channel was 0.5 mm. To improve the flow distribution, small Mylar structures were attached to the splitter using double side tape at the channel ends. The purpose of these structures is to provide mechanical support to the polyethylene splitter and prevent buckling due to the difference in sample side and carrier side flowrates.

Prior to assembly, the glass substrates were cleaned with piranha etching solution and washed with DI water. The glass substrates were also treated with glow discharge plasma (Enercon Industries Corp., LM4243-05) to make them hydrophilic which in turn facilitate easy removal of bubbles during experiments. The SPLITT channels without glow discharge showed only partial filling of the channel with a potential for decreased efficiency.

The SPLITT channel was assembled by placing the channel laminates between glass substrates and fastening the resultant assembly between two plexiglass blocks with 16 bolts with a torque wrench (PROTO-J6177F, 30 kg cm). Standard fluidics fittings and tubing were used to complete the flow assembly for the diffusional SPLITT system.

Fig. 3 shows the experimental setup for the flow arrangement. Two syringe pumps in infusion mode (KDS 100, KD Scientific) were used to pump carrier and particles solution through inlets a' and b'. Outlets of the SPLITT system were connected to two identical UV detectors (1.2 μl Model 520 UV/VIS, ESA Inc.) operating at 200 nm wavelength with 7 cm long and 0.030 in. inside diameter tubing. One more syringe pump (KDS 200), in withdraw mode, was connected to *outlet a* to control the outlet flowrates with the other outlet left open to the atmosphere. A microliter syringe (777, Hamilton) was used to inject sample with an in-line T-injector as shown in Fig. 3. The fraction collected from the outlets was determined based on the area under the absorbance peak (Peakfit Software) obtained for the respective elutions.

3.3. Pluronic treatment

After assembling the SPLITT system, a 50 mM Pluronic solution (BASF, Material 30085093) was continuously passed through the system at 0.1 ml/min for 24 h and then the channel is left at room

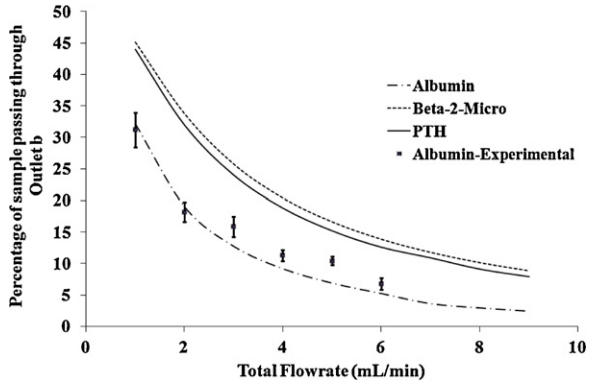

Fig. 4. (1) Plot showing the simulation results for the change in percentage of sample eluting from *outlet b*′ for albumin, β2M, and PTH (inlet ratio: 3/10; outlet ratio: 1/2) with total flowrate of 4 mL/min. (2) Experimental data for albumin.

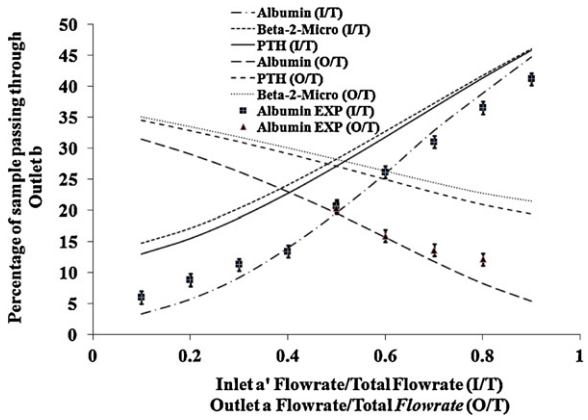

Fig. 5. Plot showing the simulation results for the change in percentage of sample eluting from *outlet b* (total flowrate: 4 ml/min; outlet ratio: 1/2) with the ratio of inlet sample to buffer flowrates (inlet ratio). (2) Plot showing the simulation results of a change in percentage of sample eluting from *outlet b* (total flowrate: 4 ml/min; inlet ratio: 1/2) with outlet flowrate fraction. (3) Experimental data for albumin.

temperature for 24 h. Pluronic treatment helps reduce undesirable protein adsorption on the channel and tubing walls.

3.4. Materials and chemicals

Aqueous PBS buffer solution (pH 7.4) was used as carrier for all the experiments done in this work. The HSA (A9771, Sigma) concentration used for these experiments was 3 mg/ml (PBS buffer). Similarly, β2-Microglobulin (M4890, Sigma–Aldrich) and parathyroid hormone (P3796, sigma) solutions were prepared at 3 mg/ml concentrations. The HSA concentration for the continuous purification experiments was 0.5 mg/ml.

4. Results and discussion

4.1. Modeling results

A wide variety of simulations were completed to help researchers understand the competing processes going on in the diffusional SPLITT system. Overall, these models showed good agreement with experimental results. The models also showed that the velocity profile in the SPLITT channel was always laminar and essentially no turbulent mixing should occur.

In the first group of simulations, the amount of sample eluting from the outlets of SPLITT system was estimated by integrating concentration across the defined outlet boundary. In diffusional SPLITT the aim is to eliminate as much β2M and PTH as possible from *oulet b*. Therefore the results in this paper were plotted with the *y* axis as a percentage of samples passing through *outlet b*.

Fig. 4 shows a graph representing the percentage of sample eluting from *outlet b* for several values of total flow rates with inlet ratio and outlet ratio set at 3/10 and 1/2. When the inlet ratio and the outlet ratio are constant, the distance between the ISP and the OSP will remain constant (i.e. the width of transport region will be constant). Therefore in such circumstances, if the total flow rate is increased, residence time of the sample decreases causing a shorter diffusion length. Therefore, the percentage of sample eluting from *outlet b* will be in the same order as that of diffusion constants: β2M > PTH > HSA.

On other hand, the inlet ratio determines the position of the ISP in the channel. If the total flowrate and outlet ratio are kept constant and inlet ratio is varied, the width of the transport region will completely depend on the inlet ratio. In this case, when the inlet ratio is small, the width of the transport region will be narrow whereas for the larger inlet ratio values it becomes broader. Therefore, when the inlet ratio is small the percentage of sample eluting from *oulet b* will be large as shown in Fig. 5 (specifically the data with (I/T) labels).

The width of the transport region can also be modified by varying the outlet ratio. Fig. 5 and specifically the results labeled with "(O/T)" represent the percentage of the sample eluting from *outlet b* for different outlet ratios with the inlet ratio kept constant at 1/2. This data looks like a mirror reflection of data labeled with (I/T) representing simulations where the inlet flow rate ratio is changing, because if the outlet ratio is increased the distance between ISP and OSP increases whereas when the inlet ratio is increased the distance between ISP and OSP decreases, increasing the likelihood a particle will make it across the transport region.

4.2. Experimental testing of the SPLITT system

The main goal of this work is to determine a viable methodology to remove β2M and PTH with the minimum loss of HSA. As the diffusivities of β2M and PTH are higher than HSA, the total flowrate for the diffusional SPLITT is chosen so that the minimum amount of HSA diffuses across the transport region and elutes out of the waste outlet (*outlet b*). Unlike H-filter devices [24] that rely on diffusion and which have a similar schematic structure to a SPLITT system, but with the thinnest dimension of the channel in the *z*-direction (SPLITT has the thinnest dimension of the channel in the *y*-direction), and which are often confused with SPLITT, the amount of time spent by sample in the SPLITT channel is a critical parameter for diffusional SPLITT function. If the total flow rate is too slow, then too much HSA is able to diffuse into the waste *outlet b*. In such a scenario, the ratio of HSA obtained from outlets will always be equal to ratio of outlet flow rates as it gets uniformly dispersed across the SPLITT channel. In contrast, if the total flow rate is extremely high it is possible to collect all HSA through *outlet a*. However, this may limit the removal of smaller proteins because there will not be enough time for any sample to diffuse across the transport region. For this reason, the initial experiments were designed to optimize total flow rate so that most of the HSA elutes out of *outlet a* with a significant proportion of the other molecules eluting out of waste outlet, *outlet b*.

In the initial experiments, sample was injected once every run into inlet a′ with buffer solution passing through both inlets continuously. This sample gets diluted in the channel and elutes out from outlets a and b and then goes to the respective detectors. The area under the absorbance peaks measured from detectors connected to *outlet a* (Area *a*) and *outlet b* (Area *b*) represent the number of particles that elute from a specific outlet. Fig. 4 shows results from

experiments using albumin (labeled "Albumin experimental") as a plot of the percentage of HSA eluting from *outlet b* calculated by (Area *b*) × 100/(Area *a* + Area *b*) for different total flow rate runs. For these experiments, the ratio of inlet flow rates (*inlet a′*/*inlet b′*) is kept constant at 3:7 (inlet ratio: 3/10) and outlet flow rates are kept equal (outlet ratio: 1/2). In these experiments, the distance between the ISP and the OSP, known as the transport region, will remain constant even with a varying total flow rate. Only the time for the sample to diffuse across the transport region will be changing as the total flowrate changes.

At smaller total flow rates, HSA disperses across the entire transport region of the channel. Hence, the absorbance ratios will be closer to 0.5 (50%). As the total flow rate is increased, the percentage of HSA diffusing across the transport region and eluting from *outlet b* is decreased. This improvement with an increase in total flow rates can be used to increase the overall throughput, if required. Experiments were repeated three times to check the repeatability of the results. The error bars were calculated such that data shows the average ± 2 standard deviations. The maximum variation found in the results was less than 15%. After analyzing the initial results, the total flow rate of 4 ml/min was chosen as only 11% of the total HSA was lost through the waste outlet, *outlet b*. This loss can be further reduced by increasing the width of the transport region (but at a cost of reduction in the efficiency of the system for removing smaller molecules), which in turn can easily be implemented by varying the inlet ratio or outlet ratio. Solid lines in Fig. 4 represent the data obtained from the numerical simulations. Fig. 4 shows that simulation results and experimental results match very well. For larger total flow rates, the experimental values for percentage of particles eluting out of *outlet b* were higher than the values obtained in the simulations. These deviations are a result of mixing and other instrumentation problems, which are not considered in this model as they vary from one device to another.

4.3. Effect of inlet flow rate ratio

Varying the inlet flow rates, while keeping outlet flow rates and the total flow rate constant, will change the thickness of the transport region. The resolution of separation is dependent on the width of the transport region; therefore, optimization of inlet flowrates is crucial for good purification. Data labeled as "Albumin exp (I/T)" in Fig. 5 shows the variation in the percentage of particles eluting out from *outlet b* as a function of inlet ratio. The maximum experimental error found in these experiments was less than 9%.

For small inlet ratio values, the width of the transport region will be large; therefore, small inlet ratio values with relatively high flow rates (4 ml/min) will cause only a small amount of the desired materials to elute out of *outlet b*. When the inlet ratio is equal to 0.5, the ISP and OSP coincide with each other and there will be no transport region. When this ratio is more than 0.5, even if the samples do not diffuse at all, some of the sample will still elute from *outlet b* as the ISP stretches into the OSP.

The solid line labeled Albumin (I/T) in Fig. 5 represents the modeling results. From Fig. 5, one can see that when the inlet ratio becomes large the modeling results do not match the experimental results. At these very low flow rates, there is a higher probability of some destabilization of the inlet flow, causing mixing and elution from *outlet b*. During experiments, it has also been observed that the percentage of particles reaching *outlet b* cannot be reduced to less than 5% due to instrumentation errors (which may be correctable with better instrument design). For very small flow rates, experimental results actually started reversing i.e. more particles eluted out from *outlet b*. Modeling results did not confirm this trend, meaning that there are unknown wall or mixing effects, which are forcing particles away from the wall. These wall effects are very complex and this paper will not consider them.

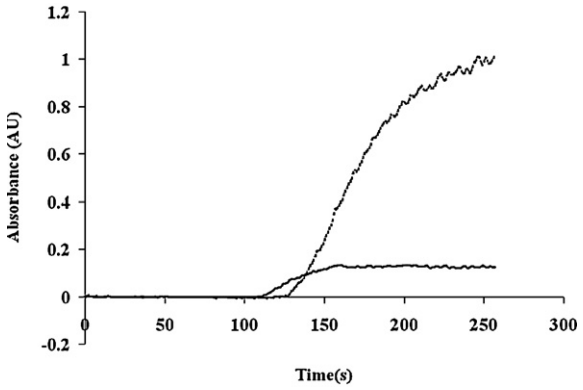

Fig. 6. Detector responses from outlets *a* and *b* (total flowrate: 4 ml/min; inlet ratio: 1/10; outlet ratio: 1/2) for experiments with albumin injected continuously through *inlet a′*.

4.4. Effect of outlet flow rate ratio

Varying outlet flow rates while keeping inlet flow rates equal and constant can also modify the transport region. The data labeled with "Albumin exp (O/T)" in Fig. 5 show the effect of outlet ratio on the percentage of particles eluting from *outlet b* compared to the total particles injected.

If the outlet ratio is increased, the width of the transport region increases, which causes less sample to elute from *outlet b*. Hence, HSA can be forced to pass through *outlet a* by using large outlet ratio values. The results obtained in these experiments are a mirror image to the ones obtained varying inlet ratios as explained previously when discussing the mathematical model. These results match closely with the modeling results which are represented as solid curves with O/T labels in Fig. 5.

4.5. Continuous small protein removal

Experiments conducted by passing protein solutions continuously through *inlet a′*, with buffer solution passing through *inlet b′* showed similar results as found in previous experiments when a concentrated sample has been injected sequentially. Fig. 6 shows the responses of detectors connected to *outlet a* and *outlet b* when the experiment was conducted with flowrates of 0.4 ml/min, 3.6 ml/min, 2 ml/min and 2 ml/min through *inlet a′*, *inlet b′*, *outlet a* and *outlet b* respectively. The HSA concentration was 0.5 mg/ml.

This plot clearly demonstrates that the UV detector response of *outlet a* was almost 9 times greater than *outlet b* which corresponds to 9 times higher concentration through *outlet a* than *outlet b*. This closely matches with the experimental results obtained using sequential sample injection. Thus, the percentage of HSA maintained in *outlet a* is at least 90%.

4.6. Parathyroid hormone (PTH) and β_2-microglobulin (β2M)

Continuous flow experiments similar to the ones used for HSA were also run using PTH and β2M with the same operating parameters as used for the HSA experiment. The percentage of β2M and PTH collected through *outlet b* were 24.6% and 18.8%. Hence, significantly larger amount of smaller molecules can be collected at *outlet b* than HSA for the same operating conditions. In the present case, nearly triple the percentage of β2M and double the percentage of PTH was removed compared to HSA. These results suggest that diffusional SPLITT systems may be useful in eliminating dangerous toxins such as β2M and PTH without losing a significant amount of HSA.

5. Conclusion and future work

A 2-dimensional numerical model was developed for diffusional SPLITT and used to optimize operational parameters. A diffusional SPLITT system was fabricated using thin plastic sheets cut with a knife plotter and was used to remove HSA, β2M and PTH proteins. The device has shown lot of promise and was able to retain most HSA and eliminate considerable amounts of β2M and PTH. The experimental results obtained using this device matched well with the mathematical model. The deviations between experimental results and the mathematical model can be attributed to mixing and instrumental errors such as sharp corners of the splitter, where there is a chance of mixing. Also if the splitter is made up of biocompatible metallic material with high modulus, then there will be little chance of bending at higher flowrates. These instrumental problems can be solved in the future. If these diffusional SPLITT systems are used in series, further increases in purification efficiency can be obtained, albeit with significant sample dilution. Clearly, this technique needs to be tested with real samples and more complex mixtures of proteins, including samples similar to uremic blood. This system is also yet to remove toxins from a uremic blood sample and significant work still remains for the system to be considered as an addendum to hemodialysis machines.

References

[1] J.C. Giddings, Sep. Sci. 1 (1996) 123.
[2] J.C. Giddings, Anal. Chem. 58 (1986) 2052.
[3] N. Narayanan, A. Saldanha, B.K. Gale, Lab Chip 6 (2006) 105.
[4] Y. Gao, M.N. Myers, B.N. Barman, J.C. Giddings, Part. Sci. Technol. 9 (1991) 105.
[5] W. Kim, M. Park, D.W. Lee, M.H. Moon, H. Lim, S. Lee, Anal. Bioanal. Chem. 378 (2004) 746.
[6] C.B. Fuh, M.N. Myers, J.C. Giddings, Ind Eng. Chem. Res. 33 (1994) 355.
[7] C.B. Fuh, M.N. Myers, J.C. Giddings, J. Microcolumn Sep. 9 (1997) 205.
[8] S. Levin, M.N. Myers, J.C. Giddings, Sep. Sci. Technol. 24 (1989) 1245.
[9] S. Merugu, N. Narayanan, B.K. Gale, Proceedings of MicroTAS 2003, Lake Tahoe, CA, 2003.
[10] R.M. Wingo, C. Prenger, M.D. Johnson, J.A. Waynert, L.A. Worl, T. Ying, Sep. Sci. Technol. 39 (2004) 2769.
[11] C.B. Fuh, J.Z. Lai, C.M. Chang, J. Chromatogr. A 923 (2001) 263.
[12] http://www.uniprot.org/uniprot/P61769 (accessed 27.01.12).
[13] http://www.uniprot.org/uniprot/P01270 (accessed 27.01.12).
[14] Y.D.S.C. Van, B. Honhon, J.M. Vandenbroucke, J.P. Huaux, H. Noel, B. Maldague, Adv. Nephrol. 17 (1988) 401.
[15] J. Floege, G. Ehlerding, Nephron 72 (1996) 9.
[16] M. Jadoul, C. Garbar, H. Noel, J. Sennesael, R. Vanholder, P. Bernaert, Kidney Int. 51 (1997) 1928.
[17] M.S. Gilbert, A. Robinson, A. Baez, S. Gupta, S. Glabman, M. Haimov, J. Bone Joint Surg. 70 (1998) 1145.
[18] S. Hara, Y. Ubara, K. Arizono, H. Ikecuchi, H. Katori, A. Yamada, Y. Ogura, H. Murata, N. Mimura, Proceedings of International Conference on New Actions of Parathyroid Hormone, vol. 21, 1995, p. 72.
[19] M. Rahimian, R. Sami, F. Behzad, Saudi J. Kidney Dis. Transplant. 19 (2008) 116.
[20] P.S. Williams, S. Levin, T. Lenczycki, J.C. Giddings, Ind. Eng. Chem. Res. 31 (1992) 2172.
[21] S. Vogel, Life's Devices: The Physical World of Animals and Plants, 1st ed., Princeton University Press, Princeton, 1988.
[22] A. Relini, C. Canale, S.D. Stefano, R. Rolandi, S. Giorgetti, M. Stoppini, A. Rossi, F. Fogolari, A. Corazza, G. Esposito, A. Gliozzi, V. Bellotti, J. Biol. Chem. 281 (2006) 16521.
[23] J.C. Hand, P. Liu, S.M. Dinh, Proceedings of AAPS Pharmsci., New Orleans, LA, 1999.
[24] P. Yager, T. Edwards, E. Fu, K. Helton, K. Nelson, M.R. Tam, B.H. Weigl, Nature 442 (2006) 412.